

# CHEMISTRY

---

## AN ASIAN JOURNAL

www.chemasianj.org

### Accepted Article

**Title:** Precise Labelling and Tracking Lipid Droplet in Adipocytes Using a Luminescent ZnSalen Complex

**Authors:** Juan Tang, Yanfei Zhang, Hao-Yan Yin, Guoheng Xu, and Jun-Long Zhang

This manuscript has been accepted after peer review and appears as an Accepted Article online prior to editing, proofing, and formal publication of the final Version of Record (VoR). This work is currently citable by using the Digital Object Identifier (DOI) given below. The VoR will be published online in Early View as soon as possible and may be different to this Accepted Article as a result of editing. Readers should obtain the VoR from the journal website shown below when it is published to ensure accuracy of information. The authors are responsible for the content of this Accepted Article.

**To be cited as:** *Chem. Asian J.* 10.1002/asia.201701010

**Link to VoR:** <http://dx.doi.org/10.1002/asia.201701010>

A Journal of



A sister journal of *Angewandte Chemie*  
and *Chemistry – A European Journal*

---

WILEY-VCH

# Precise Labelling and Tracking Lipid Droplet in Adipocytes Using a Luminescent ZnSalen Complex

Juan Tang,<sup>a+</sup> Yanfei Zhang,<sup>b+</sup> Hao-Yan Yin,<sup>a</sup> Guoheng Xu<sup>b\*</sup> and Jun-Long Zhang<sup>a\*</sup>

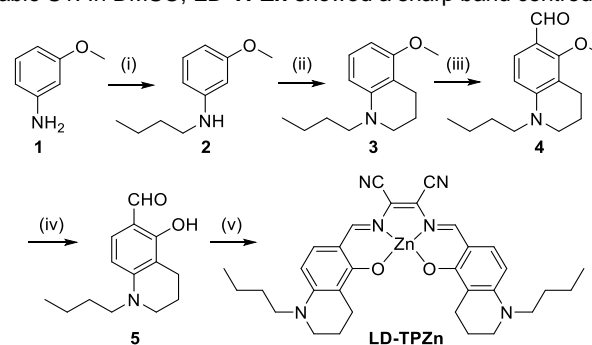
Dedicated to Professor Chi-Ming Che on the occasion of his 60th birthday

**Abstract:** Designing two-photon probes for precise labelling lipid droplet (LD) and monitoring LD dynamics in adipocytes is of great significance to understand LD homeostasis. We herein report that a luminescent metal complex **LD-TPZn** can specifically image LDs in adipose cells and tissue using one- or two-photon fluorescence microscopy. Importantly, **LD-TPZn** exhibited higher specificity to LD than commercial Nile Red and Bodipy 493/503, probably due to different cellular uptake pathways, clathrin-mediated endocytosis and non-selectively passive diffusion, respectively. More importantly, **LD-TPZn** can be applied as a two-photon LD probe to image adipose tissue, one of the most challengeable tissues for traditional one-photon fluorescence microscope imaging due to the strong light scattering. Most importantly, **LD-TPZn** can be used to monitor LD growth during adipogenesis of preadipocytes, which is highly desirable to unravel the relationship between LD homeostasis and metabolic diseases.

Cytosolic lipid droplet (LD) is a well-known organelle for cellular lipids storage, featured with a hydrophobic lipid core surrounded by a phospholipid monolayer.<sup>[1]</sup> LD has long been considered to be much less important than other organelles such as Golgi apparatus, mitochondria, etc., until recent studies suggested the close association of LD homeostasis with many diseases such as Alzheimer's disease, type 2 diabetes and cardiovascular diseases.<sup>[2]</sup> Thus, to conveniently visualize and monitor the dynamics of LDs in living cells in real time by fluorescence microscopy attracts increasing attention.<sup>[3]</sup> Generally, fluorescent LD probes were constructed by attachment of lipophilic conjugates, which have a high affinity to the hydrophobic lipid core, to organic fluorophores. Following this strategy, several LD probes have been reported such as Nile Red,<sup>[4]</sup> Bodipy 493/503,<sup>[5]</sup> LD-540,<sup>[6]</sup> Oil Red O<sup>[7]</sup> and other Sudan stains,<sup>[8]</sup> and LipidGreen,<sup>[9]</sup> contributing to unravel the underlying complexities and regulatory mechanisms of intracellular LDs. However, some important issues such as low LD specificity and strong light scattering for the adipose tissue imaging, still remained to be addressed during monitoring of LD dynamics. For instance, the widely used LD trackers Nile Red and Bodipy 493/503 suffered

from low specificity probably due to non-selectively passive diffusion.<sup>[2b, 4]</sup> Oil Red and Sudan Black only stain fixed cells.<sup>[7, 11]</sup> Moreover, recently reported LD probes such as LD-540<sup>[6]</sup>, LipidGreen,<sup>[9]</sup> monodansylpentane,<sup>[12]</sup> Seoul-Fluor,<sup>[13]</sup> FLUN-550,<sup>[14]</sup> DPH<sup>[15]</sup> and AIE luminogens,<sup>[16]</sup> used short-wavelength excitations (<500 nm), which have not been applied to image adipose tissue for its strong light scattering with severe refractive index mismatches.<sup>[17]</sup> Only recently, Rendina et al. reported a new carborane-containing coumarin which could selectively stain lipid droplets in live adipocytes.<sup>[18]</sup> To address these issues, we herein report the design of a luminescent ZnSalen complex specific to stain LD and monitor the dynamics, and capable of two-photon excitation to circumvent the strong light scattering.<sup>[19]</sup>

Luminescent metal complexes are emerging biological probes for the intriguing photophysical properties and unique chemical structures.<sup>[20]</sup> For LD imaging, a Re tetrazolato complex<sup>[21]</sup> and a alkynyl gold(I) cluster<sup>[22]</sup> have previously been reported, yet suffering from poor photostability and potential cytotoxicity arising from heavy metals. In this work, we chose bioavailable Zn<sup>2+</sup> ion as metal centre supported by luminescent Salen ligand, which has been applied as fluorescent metal probes in cell imaging.<sup>[23]</sup> A notable bonus to such metal probes is the opportunity to modulate cellular uptake pathway and subcellular localization by fine-tuning intermolecular interaction between metal and ligand.<sup>[23b-d]</sup> To stain the hydrophobic interior of LD, we used aliphatic chain modified N-substituent salicylaldehyde, and synthesized a luminescent ZnSalen (Salen= 2,3-bis[(1-butyl-5-hydroxy-1,2,3,4-tetrahydroquinoline-6-methyl ene)amino]but-2-enedinitrile) complex (**LD-TPZn**), as shown in Scheme 1. This complex was fully characterized by <sup>1</sup>H-NMR, HR-ESI, and IR spectroscopies and spectrometers (detailed synthesis and characterization were listed in supporting information). Photophysical data were shown in Fig. 1a and Table S1. In DMSO, **LD-TPZn** showed a sharp band centred at



**Scheme 1.** Synthetic route for LD specific **LD-TPZn**. (i) 1-butyl bromide,  $\text{KHCO}_3$ ,  $\text{CH}_3\text{CN}$ ,  $95^\circ\text{C}$ , 16 h, 60%; (ii)  $\text{BrCH}_2\text{CH}_2\text{CH}_2\text{Br}$ ,  $\text{KHCO}_3$ ,  $\text{CH}_3\text{CN}$ ,  $95^\circ\text{C}$ , 16 h, 30%; (iii)  $\text{POCl}_3$ , DMF,  $0^\circ\text{C}$  to r.t., 30 min; followed by hydrolysis in icy water, 90 min, 43%; (iv)  $\text{BBr}_3$ , dry  $\text{CH}_2\text{Cl}_2$ ,  $-78^\circ\text{C}$  to r.t., 2 h, 90%; (v) 2,3-diaminomaleonitrile,  $\text{Zn}(\text{OAc})_2 \cdot 2\text{H}_2\text{O}$ , ethanol,  $90^\circ\text{C}$ , 24 h, 70%.

[a] Dr. J. Tang,<sup>+</sup> H. Y. Yin, Prof. J. L. Zhang  
Beijing National Laboratory for Molecular Sciences, State Key Laboratory of Rare Earth Materials Chemistry and Applications, College of Chemistry and Molecular Engineering, Peking University, Beijing 100871, P.R. China, Fax: +86-10-62767034.  
E-mail: zhangjunlong@pku.edu.cn.

[b] Y. F. Zhang,<sup>+</sup> Prof. G. H. Xu<sup>\*</sup>  
Department of Physiology and Pathophysiology, School of Basic Medical Sciences, Peking University, Beijing 100191, P.R. China, Fax: +86-10-62767034.  
E-mail: xug@bjmu.edu.cn.

[+ ] These authors contributed equally to this work.

Supporting information for this article is given via a link at the end of the document.

## COMMUNICATION

WILEY-VCH

390 nm with a shoulder at 440 nm assigned to  $\pi$ - $\pi^*$  transition, and a low-energy band centred at 599 nm. It displayed an intense red fluorescence with emission (600-700nm) centred at 637 nm and a quantum yield of 0.44. **LD-TPZn** exhibited a two-photon absorption cross section ( $\delta$ ) of ca. 110 GM at 880 nm, using Rhodamine B as the reference (Fig. S1). To estimate the lipophilicity of **LD-TPZn**, we carried out inductively coupled plasma-atomic emission spectrometer (ICP-AES) to access the logarithm of the n-octanol/water partition coefficient (Log *P*), giving a value of  $1.8 \pm 0.1$ . The calculated cLog *P*<sup>[24]</sup> value is 8.2, close to those of reported LD probes<sup>[13b]</sup>.

To demonstrate the capability of **LD-TPZn** to bind LD, we prepared an artificial oil-in-water emulsion system to mimic LD, where the interior consists of hydrophobic lipid wrapped in an amphiphilic phospholipid monolayer. As shown in Fig. 1b-c, **LD-TPZn** (10  $\mu$ M) has very weak emission in PBS (pH 7.4), probably due to the aggregation of **LD-TPZn**. Titration of oil-in-water emulsion (10 mg·mL<sup>-1</sup>) to the above PBS solution (pH 7.4)

resulted a gradual fluorescence increase (up to 5-fold enhancement after addition of 20  $\mu$ L emulsion). Furthermore, 3D reconstructed imaging by confocal laser scanning microscopy (CLSM) (Fig. 1d-e) showed that red fluorescence of **LD-TPZn** distributed homogeneously inside the emulsion, giving a red solid structure. To better elucidate the ability of **LD-TPZn** to stain hydrophobic component, we prepared a liposome system with an aqueous interior surrounded by an amphiphilic phospholipid bilayer and observed **LD-TPZn** only staining the phospholipid bilayers. No fluorescence was found in the aqueous interior, leading to a red hollow structure (Fig. 1f-g). Finally, we applied **LD-TPZn** to stain freshly extracted lipid droplets from mature adipose cells. 2D fluorescence imaging showed the uniform red-color round lipid droplets (Fig. S2). Thus, these cell-free studies clearly suggested that **LD-TPZn** could accumulate in the hydrophobic interior of lipid droplets accompanied with a "turn-on" fluorescence driven by its lipophilicity.

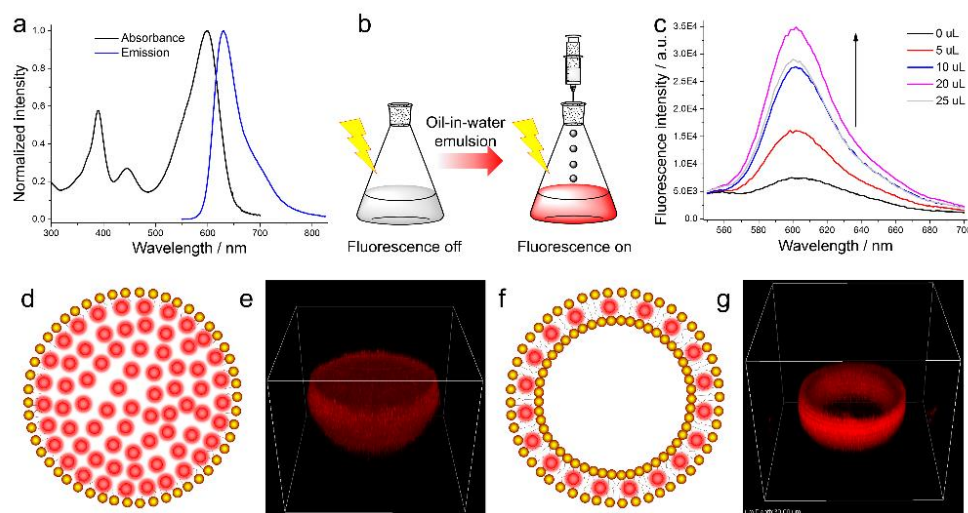


**Figure 1.** (a) Normalized UV-vis and fluorescence spectra of **LD-TPZn** in DMSO,  $\lambda_{ex}$  = 450 nm. (b) Oil-in-water emulsion-enhanced fluorescence of **LD-TPZn** in PBS (pH 7.4); (c) Titration of oil-in-water emulsion to **LD-TPZn** in PBS (pH 7.4) monitored by fluorescence spectra; (d, f) Schematic diagram of **LD-TPZn** staining of (d) oil-in-water emulsion and (f) liposome; (e, g) 3D reconstructed imaging of **LD-TPZn** by CLSM in (e) oil-in-water emulsion (width 36.27  $\mu$ m, height 36.27  $\mu$ m, depth 30.00  $\mu$ m) and (g) liposome (width 33.41  $\mu$ m, height 33.41  $\mu$ m, depth 30.00  $\mu$ m).

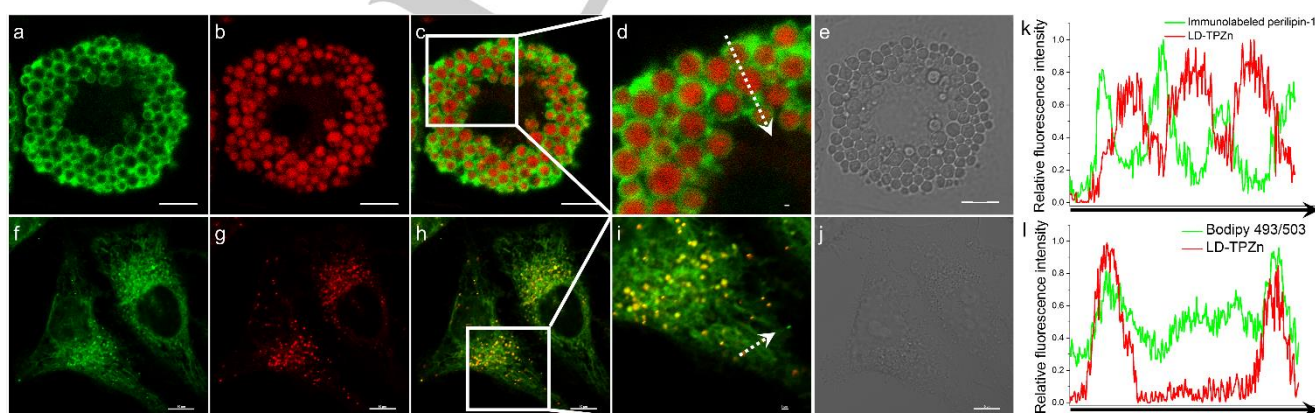


**Figure 2.** Co-localization imaging of **LD-TPZn** (a-e) with immunolabeled perilipin-1 in adipose cells or (f-j) with Bodipy 493/503 in HeLa cells. Cells were treated with 2  $\mu$ M of **LD-TPZn** for 2 h. Fluorescence images of (a) immunolabeled perilipin-1 or (f) Bodipy 493/503; (b and g) Fluorescence images of **LD-TPZn**; (c and h) Merged images of (a-b) and (f-g), respectively; (e and j) Differential interference contrast (DIC) images; scale bar = 10  $\mu$ m. (d and i) Enlarged images of the white box in (c and h), respectively; scale bar = 1  $\mu$ m; (k and l) Relative fluorescence intensity profile along the arrow in (d and i), respectively.

## COMMUNICATION

WILEY-VCH

Prior to cell imaging, the cytotoxicity and photostability of **LD-TPZn** were evaluated in HeLa cells. The CCK-8 assay showed low cytotoxicity (90% cell viability, 8  $\mu\text{M}$  **LD-TPZn**) for 24 hours (Fig. S3). Compared with commercial Nile Red, higher photostability was observed for **LD-TPZn**, which shows ca. 50% fluorescence decay in contrast to ca. 90% by Nile Red upon continuous scanning of cells by a 543 nm laser (0.91 mW) for 900 seconds (Fig. S4).

To identify the precise location of **LD-TPZn**, we conducted co-localization analysis in early-differentiated adipocytes with immunolabeled perilipin-1, which coats LDs exclusively in adipocytes.<sup>[25]</sup> As shown in Fig. 2a-e, distinct red fluorescence from **LD-TPZn** precisely located within discrete green fluorescent ring-like structures immunostained with perilipin-1. Plotting the intensity along with the arrow in Fig. 2d gave a complete inverse correlation between red fluorescence of **LD-TPZn** and green fluorescence of immunolabeled perilipin-1 (Fig. 2k). These results strongly suggested that **LD-TPZn** specifically localize in the hydrophobic core of LDs. We then examined subcellular localization of **LD-TPZn** in HeLa cells using commercial Bodipy 493/503 as a control LD tracker. As shown in Fig. 2f-j, **LD-TPZn** displayed the globular red fluorescence with a size ranged from 300 to 600 nm, which was included in green fluorescence region of Bodipy 493/503. However, Bodipy 493/503 showed a more diffused fluorescence over the cytoplasm, not only limited to LDs (yellow spots) but also to other reticular structures (green emission) of intracellular membranes and organelles (Fig. 2h). As shown in Fig. 2l, **LD-TPZn** displayed low background, whereas the control Bodipy 493/503 showed high-baseline intensity profile. Thus, the above results demonstrated a higher specificity of **LD-TPZn** toward LDs than Bodipy 493/503.

Cellular uptake is important to the post-internalization fate and intracellular location of the cargoes.<sup>[26]</sup> The classical commercial LD probes (Nile Red and Bodipy 493/503) suffer poor LD selectivity since they passively diffuse into cells, non-selectively interact with intracellular hydrophobic components and accumulate in LDs and other hydrophobic structures such as intracellular membranes and membranous organelles.<sup>[10]</sup> Thus, directing a probe to LDs through a particular endocytosis

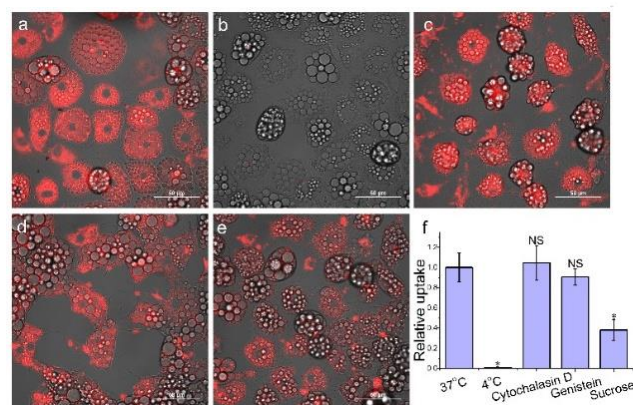


**Figure 3.** Cellular uptake of **LD-TPZn** by adipocytes. (a-e) Merged images of fluorescence images of **LD-TPZn** and differential interference contrast (DIC) images. (a) at 37°C; (b) at 4°C; (c) 1  $\mu\text{g}\cdot\text{mL}^{-1}$  cytochalasin D; (d) 100  $\mu\text{M}$  genistein; (e) 450 mM sucrose. Cytochalasin D, genistein and sucrose were preincubated with cells for 30 min; scale bar: 10  $\mu\text{m}$ . (f) Mean fluorescence intensity of internalized **LD-TPZn** by adipose cell. (n=30, \*P < 0.001, NS: nonsignificant). Data were obtained by confocal imaging and calculated by ImageJ.

trafficking pathway would be a desirable approach. Previously, we reported the importance of intermolecular metal-ligand interaction of ZnSalen on the aggregation and even cellular uptake pathway of ZnSalen.<sup>[27]</sup> In this work, we performed dynamic light scattering (DLS) to assess the hydrodynamic diameters (ca. 52 nm) of **LD-TPZn** aggregates in aqueous solution (Fig. S5). To understand the cellular uptake pathway of **LD-TPZn**, we treated adipocytes at a low temperature to stall all energy-dependent active transport and applied sucrose<sup>[28]</sup>, genistein<sup>[29]</sup> or cytochalasin D<sup>[30]</sup> as endocytosis inhibitors to selectively block clathrin-mediated endocytosis, caveolae-dependent endocytosis or macropinocytosis, respectively. As shown in Fig. 3, each adipocyte has multiple lipid droplets which look like spots on the cell in the bright field images. CLSM imaging showed that 4°C-treated cells displayed weak intracellular fluorescence and the uptake level was as low as 1% of that in the 37°C-treated cells (the positive control). Sucrose-treated cells exhibited distinct weak fluorescence and the uptake was lowered to 40% of the positive control. However, both genistein and Cytochalasin D exerted no effect on the uptake of **LD-TPZn**, giving comparable intracellular fluorescence (90% and 100%, respectively) to the positive control. Since there is no possibility to form the sucrose-**LD-TPZn** adduct (Fig. S6), the above results indicated that cellular uptake of **LD-TPZn** is highly energy-dependent and via a clathrin-mediated endocytosis pathway. It is of importance on LD specificity since it could prevent possible contact of **LD-TPZn** with lipophilic structures of other organelles such as mitochondria and ER.<sup>[10]</sup>

As obesity is a growing global health problem directly related to the number and size of the adipocytes,<sup>[31]</sup> monitoring the processes of adipocytes differentiation is of pathological and

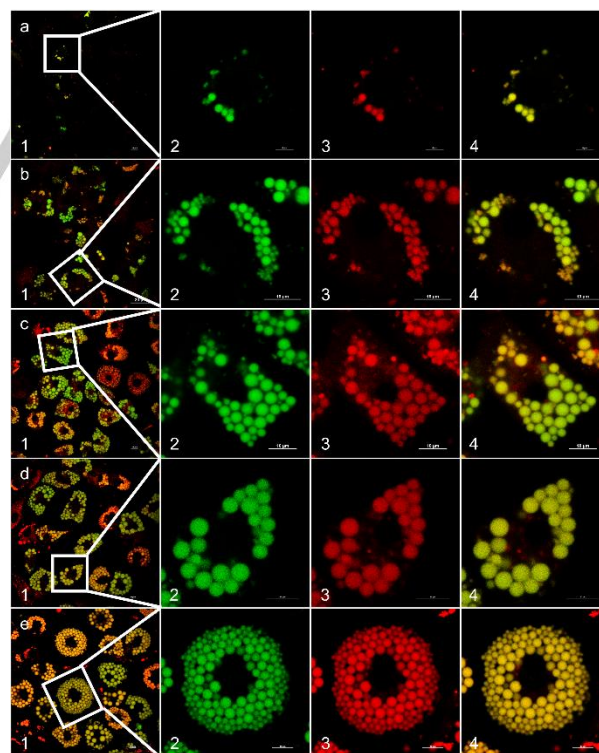


**Figure 4.** LD formation during preadipocyte differentiation: (a) day 0; (b) day 1; (c) day 2; (d) day 3; (e) day 4. (1) Images of preadipocyte in full field; (2-4) Enlarged images of white box in (1); (2) Fluorescence images of Bodipy 493/503; (3) Fluorescence images of **LD-TPZn**; (4) Merged images of (2) and (3); scale bar: 10  $\mu\text{m}$ .

physiological significance. In this work, we investigated the capability of **LD-TPZn** to monitor LD growth during adipogenesis of rat preadipocytes and used Bodipy 493/503 as the positive control. At the initiation day (day 0, Fig. 4a), **LD-TPZn** treated-fibroblast-like cells display negligible intracellular fluorescence, in addition to the occasional few red fluorescent LDs. From day 1 to day 3 (Fig. 4b-d), cells proliferated by cell division and differentiated into spherical adipocytes. The LDs that accumulated in each adipocyte grew from less than 1  $\mu\text{m}$  to more than 5  $\mu\text{m}$  in diameter during this period. However, at day 4 (Fig. 4e), the large LDs fragmented into smaller size LDs with diameter of 1-2  $\mu\text{m}$  and filled the whole cells. As shown in Fig. 4, **LD-TPZn** overlapped well with Bodipy 493/503 during the process. These results highlight the potential application of **LD-TPZn** in tracking LD biogenesis during adipogenesis of preadipocytes.

Adipose tissue is one of the most challenging tissues for traditional fluorescence imaging due to its highly scattering feature with severe refractive index mismatches.<sup>[17]</sup> To address this issue, two-photon fluorescence microscopy is alternative to

image LDs within adipose tissue for the less sensitivity to light scattering, making high-resolution deep imaging possible.<sup>[19]</sup> Due to moderate two-photon absorptions cross sections across 790-880 nm spectral window (up to 110 GM) (Fig. S1), **LD-TPZn** was firstly investigated at cell level in two-photon confocal imaging, using a 790 nm femtosecond laser and a LP 650 filter. As shown in Fig. S7, in HeLa cells, two-photon excited **LD-TPZn** displayed apparent punctate red fluorescence. Then, we performed Z-stack two-photon confocal imaging of rat subcutaneous adipose tissues using **LD-TPZn** as a bioprobe. As shown in Fig. 6a, LDs in a 130  $\mu\text{m}$ -thick adipose tissue slice emerged as many red globular structures. To demonstrate the globular structures are LDs rather than mature adipocytes, one-photon 3D reconstructed imaging was carried out using Hoechst 33342 to stain the nuclei. As shown in Fig. 6b, every mature adipocyte contained a red single globular LD with ca. 50 - 100  $\mu\text{m}$  in diameter clinging to a relative little punctate nucleus with ca. 10  $\mu\text{m}$  in diameter. Thus, two-photon imaging of LDs at adipose cell and tissue level is achievable via **LD-TPZn**.

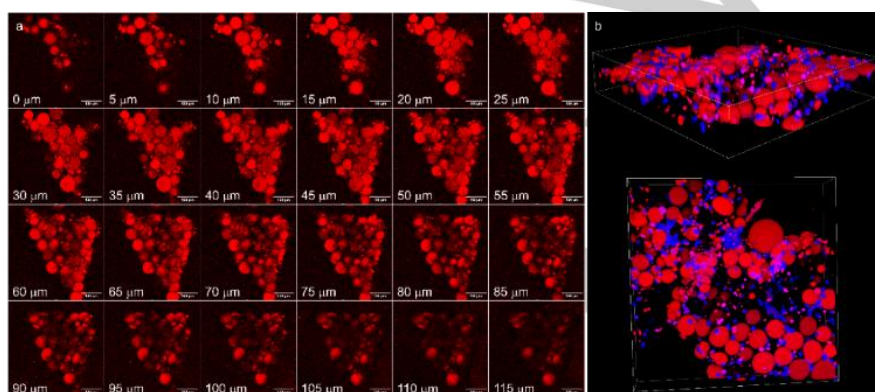


**Figure 6.** (a) Two-photon fluorescence imaging of LDs in adipose tissue slice incubated with **LD-TPZn** (2  $\mu\text{M}$ ) for 6 h; a 790 nm femtosecond laser and a LP 650 filter were used for detection of **LD-TPZn**; scale bar: 100  $\mu\text{m}$ . Labels from 0-115  $\mu\text{m}$  indicate scanning depths of the tissue slices. (b) One-photon 3D reconstructed imaging of adipose tissue stained with **LD-TPZn** (red fluorescence) and Hoechst 33342 (blue fluorescence), width 638.05  $\mu\text{m}$ , height 638.05  $\mu\text{m}$ , depth 130.50  $\mu\text{m}$ .

In conclusion, we have synthesized a new luminescent ZnSalen complex (**LD-TPZn**) and demonstrated the capability to stain LD precisely in living cells. Importantly, compared with the commercial tracker (Bodipy 493/503), **LD-TPZn** exhibited higher specificity via clathrin-mediated *endocytosis* pathway, which is related to the intermolecular metal-ligand interaction. More importantly, large two-photon absorption cross section (up to 110 GM) at 790-880 nm spectral window renders **LD-TPZn** a two-photon bioprobe for imaging LDs at even tissue level. Most importantly, **LD-TPZn** could be used for dynamic adipogenesis of preadipocytes, which demonstrated the potential application in further understanding the relationship between LD homeostasis and some metabolic diseases at cellular or even tissue levels.

## Acknowledgements

We acknowledge financial support from the National Key Basic Research Support Foundation of China (Grant 2015CB856301)

and the National Scientific Foundation of China (Grants 21571007, 21271013, 21321001, 81570791).

**Keywords:** Luminescent metal complex • lipid droplets • fluorescence microscopy • cell imaging • chemical biology

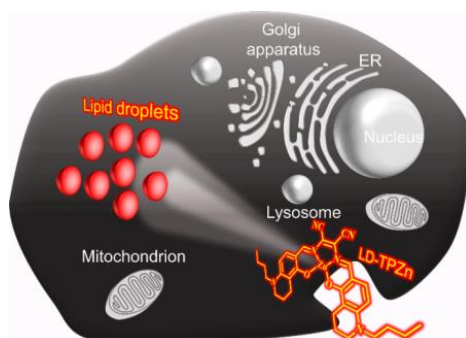
- [1] a) S. Martin, R. G. Parton, *Nat. Rev. Mol. Cell Biol.* **2006**, *7*, 373-378; b) A. R. Thiam, R. V. Farese Jr, T. C. Walther, *Nat. Rev. Mol. Cell Biol.* **2013**, *14*, 775-786.
- [2] a) Y. Guo, K. R. Cordes, R. V. Farese, T. C. Walther, *J. Cell Biol.* **2009**, *122*, 749-752; b) T. C. Walther, R. V. Farese, *Annu. Rev. Biochem.* **2012**, *81*, 687-714.
- [3] a) M. Beller, K. Thiel, P. J. Thul, H. Jäckle, *FEBS Lett.* **2010**, *584*, 2176-2182; b) M. Digel, R. Ehehalt, J. Füllekrug, *FEBS Lett.* **2010**, *584*, 2168-2175.
- [4] P. Greenspan, E. P. Mayer, S. D. Fowler, *J. Cell Biol.* **1985**, *100*, 965-973.
- [5] E. E. Spangenburg, S. J. P. Pratt, L. M. Wohlers, R. M. Lovering, *J. Biomed. Biotechnol.* **2011**, *2011*, 1-8.
- [6] J. Spandl, D. J. White, J. Peychl, C. Thiele, *Traffic* **2009**, *10*, 1579-1584.

- [7] E. J. O'Rourke, A. A. Soukas, C. E. Carr, G. Ruvkun, *Cell Metab.* **2009**, *10*, 430-435.
- [8] T. Aoki, H. Hagiwara, T. Fujimoto, *Exp. Cell Res.* **1997**, *234*, 313-320.
- [9] a) J. H. Lee, J.-H. So, J. H. Jeon, E. B. Choi, Y.-R. Lee, Y.-T. Chang, C.-H. Kim, M. A. Bae, J. H. Ahn, *Chem. Commun.* **2011**, *47*, 7500-7502; b) H. S. Pagire, H.-S. Chun, M. A. Bae, J. H. Ahn, *Tetrahedron* **2013**, *69*, 3039-3044.
- [10] a) M. E. Johnson, D. A. Berk, D. Blankschtein, D. E. Golan, R. K. Jain, R. S. Langer, *Biophys. J.* **1996**, *71*, 2656-2668; b) N. G. Turner, R. H. Guy, *J. Pharm. Sci.* **1997**, *86*, 1385-1389.
- [11] S. Fukumoto, T. Fujimoto, *Histochem. Cell Biol.* **2002**, *118*, 423-428.
- [12] H.-J. Yang, C.-L. Hsu, J.-Y. Yang, W. Y. Yang, *PLoS one* **2012**, *7*, e32693.
- [13] a) E. Kim, S. Lee, S. B. Park, *Chem. Commun.* **2012**, *48*, 2331-2333; b) Y. Lee, S. Na, S. Lee, N. L. Jeon, S. B. Park, *Mol. BioSyst.* **2013**, *9*, 952-956; c) J. Park, S. Na, Y. Lee, S. Lee, S. Park, N. Jeon, *Energies* **2013**, *6*, 5703-5716.
- [14] A. Goel, A. Sharma, M. Kathuria, A. Bhattacharjee, A. Verma, P. R. Mishra, A. Nazir, K. Mitra, *Org. Lett.* **2014**, *16*, 756-759.
- [15] J. G. Collard, A. De Wildt, *Exp. Cell Res.* **1978**, *116*, 447-450.
- [16] a) E. Wang, E. Zhao, Y. Hong, J. W. Y. Lam, B. Z. Tang, *J. Mater. Chem. B* **2014**, *2*, 2013-2019; b) M. Kang, X. Gu, R. T. K. Kwok, C. W. T. Leung, J. W. Y. Lam, F. Li, B. Z. Tang, *Chem. Commun.* **2016**, *52*, 5957-5960; c) Z. Wang, C. Gui, E. Zhao, J. Wang, X. Li, A. Qin, Z. Zhao, Z. Yu, B. Z. Tang, *ACS Appl. Mater. Inter.* **2016**, *8*, 10193-10200; d) M. Gao, H. Su, S. Li, Y. Lin, X. Ling, A. Qin, B. Z. Tang, *Chem. Commun.* **2017**, *53*, 921-924; e) M. Gao, H. Su, Y. Lin, X. Ling, S. Li, A. Qin, B. Z. Tang, *Chem. Sci.* **2017**, *8*, 1763-1768.
- [17] D. R. Larson, W. R. Zipfel, R. M. Williams, S. W. Clark, M. P. Bruchez, F. W. Wise, W. W. Webb, *Science* **2003**, *300*, 1434-1436.
- [18] A. Wu, J. L. Kolanowski, B. B. Boumelhem, K. Yang, R. Lee, A. Kaur, S. T. Fraser, E. J. New, L. M. Rendina, *Chem. Asian J.* **2017**, *12*, 1704-1708.
- [19] F. Helmchen, W. Denk, *Nat. Meth.* **2005**, *2*, 932-940.
- [20] a) K. L. Haas, K. J. Franz, *Chem. Rev.* **2009**, *109*, 4921-4960; b) K. K.-W. Lo, M.-W. Louie, K. Y. Zhang, *Coord. Chem. Rev.* **2010**, *254*, 2603-2622; c) V. Fernández-Moreira, F. L. Thorp-Greenwood, M. P. Coogan, *Chem. Commun.* **2010**, *46*, 186-202; d) Q. Zhao, C. Huang, F. Li, *Chem. Soc. Rev.* **2011**, *40*, 2508-2524; e) E. Baggaley, J. A. Weinstein, J. Williams, *Coord. Chem. Rev.* **2012**, *256*, 1762-1785; f) D. L. Ma, H. Z. He, K. H. Leung, D. S. H. Chan, C. H. Leung, *Angew. Chem. Int. Ed.* **2013**, *52*, 7666-7682; g) X. Li, X. Gao, W. Shi, H. Ma, *Chem. Rev.* **2014**, *114*, 590-659; h) J. Zhou, H. Ma, *Chem. Sci.* **2016**, *7*, 6309-6315.
- [21] C. A. Bader, R. D. Brooks, Y. S. Ng, A. Sorvina, M. V. Werrett, P. J. Wright, A. G. Anwer, D. A. Brooks, S. Stagni, S. Muzzioli, M. Silberstein, B. W. Skelton, E. M. Goldys, S. E. Plush, T. Shandala, M. Massi, *RSC Adv.* **2014**, *4*, 16345-16351.
- [22] E. I. Koshel, P. S. Chelushkin, A. S. Melnikov, P. Y. Serdobintsev, A. Y. Stolbovaia, A. F. Saifitdinova, V. I. Shcheslavskiy, O. Chernyavskiy, E. R. Gaginskaya, I. O. Koshevoy, S. P. Tunik, *J. Photochem. Photobiol. A* **2017**, *332*, 122-130.
- [23] a) J. Tang, H. Y. Yin, J. L. Zhang, in *Inorganic and Organometallic Transition Metal Complexes with Biological Molecules and Living Cells*, Academic Press, **2017**, pp. 1-53; b) J. Tang, D. Xie, H.-Y. Yin, J. Jing, J.-L. Zhang, *Org. Biomol. Chem.* **2016**, *14*, 3360-3368;
- c) J. Tang, Y.-B. Cai, J. Jing, J.-L. Zhang, *Chem. Sci.* **2015**, *6*, 2389-2397; d) J. Lai, X.-S. Ke, J. Tang, J.-L. Zhang, *Chin. Chem. Lett.* **2015**, *26*, 937-941; e) D. Xie, J. Jing, Y.-B. Cai, J. Tang, J.-J. Chen, J.-L. Zhang, *Chem. Sci.* **2014**, *5*, 2318-2327; f) C. Nie, Q. Zhang, H. Ding, B. Huang, X. Wang, X. Zhao, S. Li, H. Zhou, J. Wu, Y. Tian, *Dalton Trans.* **2014**, *43*, 599-608; g) J. Jing, J.-L. Zhang, *Chem. Sci.* **2013**, *4*, 2947-2952; h) J.-J. Chen, J. Jing, H. Chang, Y. Rong, Y. Hai, J. Tang, J.-L. Zhang, P. Xu, *Autophagy* **2013**, *9*, 894-904; i) J. Jing, J.-J. Chen, Y. Hai, J. Zhan, P. Xu, J.-L. Zhang, *Chem. Sci.* **2012**, *3*, 3315-3320; j) Y. Hai, J.-J. Chen, P. Zhao, H. Lv, Y. Yu, P. Xu, J.-L. Zhang, *Chem. Commun.* **2011**, *47*, 2435-2437.
- [24] A. K. Ghose, V. N. Viswanadhan, J. J. Wendoloski, *J. Phys. Chem. A* **1998**, *102*, 3762-3772.
- [25] D. L. Brasaemle, *J. Lipid Res.* **2007**, *48*, 2547-2559.
- [26] a) I. A. Khalil, K. Kogure, H. Akita, H. Harashima, *Pharmacol. Rev.* **2006**, *58*, 32-45; b) B. Yameen, W. I. Choi, C. Vilos, A. Swami, J. Shi, O. C. Farokhzad, *J. Control Release* **2014**, *190*, 485-499.
- [27] J. Tang, Y.-B. Cai, J. Jing, J.-L. Zhang, *Chem. Sci.* **2015**, *6*, 2389-2397.
- [28] J. E. Heuser, R. G. Anderson, *J. Cell Biol.* **1989**, *108*, 389-400.
- [29] I. R. Nabi, P. U. Le, *J. Cell Biol.* **2003**, *161*, 673-677.
- [30] C. A. Puckett, R. J. Ernst, J. K. Barton, *Dalton Trans.* **2010**, *39*, 1159-1170.
- [31] S. Heinonen, L. Saarinen, J. Naukkarinen, A. Rodriguez, G. Fruhbeck, A. Hakkarainen, J. Lundbom, N. Lundbom, K. Vuolteenaho, E. Moilanen, P. Arner, S. Hautaniemi, A. Suomalainen, J. Kaprio, A. Rissanen, K. H. Pietilainen, *Int. J. Obes* **2014**, *38*, 1423-1431.

## Entry for the Table of Contents

## COMMUNICATION

A two-photon luminescent ZnSalen complex **LD-TPZn** precisely images LDs in adipose cells and tissues due to its clathrin-mediated endocytosis pathway.



Author(s), Corresponding Author(s)\*

Page No. – Page No.

Title